PERMANENT MAGNET LINEAR ACTUATORS WITH CONCENTRATED COILS

Antonino Di Gerlando, Roberto Perini, Mario Ubaldini
Department of Electrical Engineering
Politecnico di Milano
Piazza Leonardo da Vinci, 32 – 20133 Milano, Italy
Tel: +3902239937(22-14-95) Fax: +390223993703
Emails: [antonino.digerlando, roberto.perini, mario.ubaldini]@polimi.it

***Abstract* – As known, linear actuators used for automation and industrial processes should present high performances, in terms of force amplitude, enhanced dynamic response, low cogging and reduced force ripple, small e.m.f. waveform distortion, structural simplicity, compactness and robustness, low cost.**

Achieving all these goals is not a simple task: the paper describes some configurations, design criteria and performances of a few permanent magnet (PM) actuators, whose armature structures, iron-core and toothed, are equipped with symmetrical three-phase windings made of concentrated coils, suited to fairly satisfy the described requirements.

Key words– concentrated windings, iron-core PM actuators, low cogging and torque ripple, sinusoidal E.M.F.s.

1. INTRODUCTION

During the last years, a great interest has grown towards the tooth-coil electrical machines (both rotating and linear), equipped with concentrated coils, thanks to their conspicuous constructional and functional advantages (mainly an easier machine manufacture and the development of high forces (torques) and E.M.F.s at low speeds).
Several types have been developed, mainly concerning rotating structures [1-6]. The problems usually related to an effective employment of these solutions concern the waveform of the E.M.F. and the force (torque) ripple: the approach followed till now in order to face these problems regards the analysis of the extension of teeth and poles, referred to the extension of the tooth pitches, while a general theory about the winding structures seems not developed yet.

In the paper, at first the theory of the windings equipped with concentrated coils is considered, describing suited laws for their definition [7], and showing analogies and differences with respect to the classical distributed windings.
Subsequently, the constructional and operation features of linear actuators equipped with such concentrated coil windings are analysed: reference will be made to single-side and double-side structures, discussing also the end effects affecting E.M.F. and torque waveforms, and the ways to mitigate them.
Finally, some figures of merits are proposed, for a chosen device, to characterise its performances.

2. CHARACTERISTICS OF CONCENTRATED-COIL WINDING ARRANGEMENTS

The use of tooth-coil machines exhibits numerous constructional and operating advantages:
– the concentrated coil windings are inherently better arranged, for the absence of endwindings superposition;
– the tooth coil endwindings are very short, with significant saving of copper mass and reduction of winding losses;
– the use of coils facilitates the winding construction: in case of open slots, it is also possible and convenient to construct the coils separately, subsequently disposing them around the teeth and completing the winding connections.

In the following just the general characteristics of the tooth-coil machines in one electromagnetic cycle will be shown, for now disregarding the end effects occurring in the linear machines.

Fig.1 shows a portion of a device example, suited to describe the general features of the tooth-coil machines. Common characteristics of these machines are:
– uniformly distributed magnetic structures of armature and inductor (each structure has equally shaped saliencies);
– absence of skewing among teeth and PMs;
– almost equality among tooth pitch τ_t and PM pitch τ_m (it can be $\tau_m<\tau_t$ or $\tau_m>\tau_t$, but $\tau_m \neq \tau_t$);
– in case of double-layer winding (whose performances are generally better than those of single-layer windings), identity among the layers, even if displaced (disregarding directions);
– in case of all teeth wound, series inverted connection of coils around adjacent teeth of the same phase (and disposed in the same layer): this configuration is defined controverse winding;
– in case of alternatively teeth wound (not in fig.1), series connection of adjacent coils of the same phase (and of the same layer): this configuration is defined equiverse winding.

The following definitions and properties are valid (see fig.1):

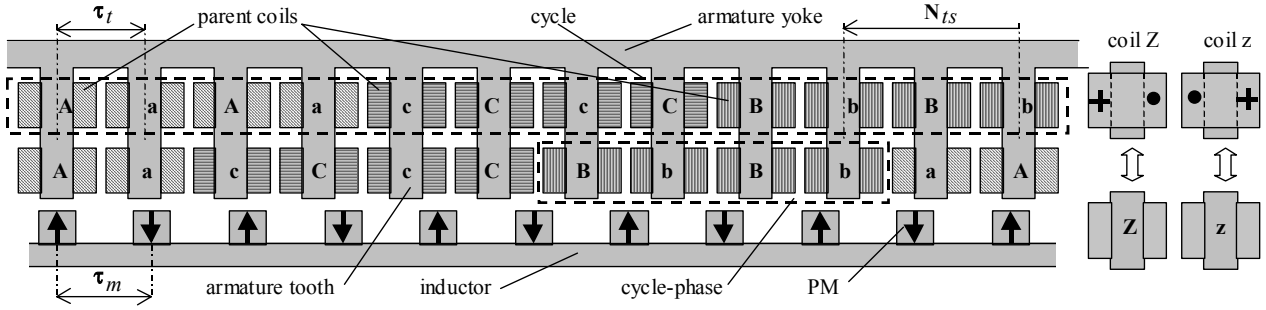

Figure1. Left: device portion, with single-side PM inductor and armature structure with double-layer winding ($N_{tc} = N_{cc} = 12$; $N_{mc} = 11$; $N_{ts} = 2$); right: equivalent simplified representation of phase Z coils (Z = A, B, C) around armature teeth, according to the two possible coil dispositions.

– cycle: space period, i.e. periphery portion at which bounds the faced structures show the same reciprocal disposition;
– cycle-phase: referring to a layer, portion of one cycle including adjacent coils belonging to the same phase;
– the N° of armature teeth/cycle N_{tc} and the N° of armature coils/cycle N_{cc} must be multiple of the N° of phases N_{ph}; for controverse windings: $N_{ccph} = N_{tcph}$ (N_{tcph} = any integer); for equiverse windings: $N_{ccph} = N_{tcph}/2$ (N_{tcph} = even);
– as concerns the N° of armature teeth/(cycle-phase) N_{tcph} and the N° of armature coils/(cycle-phase) N_{ccph}, the following relations are valid: $N_{tc} = N_{ph} \cdot N_{tcph}$; $N_{cc} = N_{ph} \cdot N_{ccph}$;
– it can be shown that, in order to obtain the maximum winding factor, the N° of PMs/cycle N_{mc} should differ by 1 with respect to N_{tc}; thus, one of the following cases can be chosen: $N_{mcs} = N_{tc} + 1$ (s: superior), or $N_{mci} = N_{tc} - 1$ (i: inferior);
– all the cycles are identical: thus, the maximum N° of parallel paths of each phase equals the N° of cycles N_c.

Considering for now just one layer, called Z, z the generic Z phase armature coils (Z = A, B, C; z = a, b, c, see fig.1 right), in order to assign the coils to the phases, the electrical angles must be considered (being 180^e the electrical angle among adjacent PMs); apart from the winding sense, the angle α_t among adjacent teeth equals: $\alpha_t = 180^e \cdot (N_{mc}/N_{tc})$; thus, we have:

– coil sequence of a cycle-phase: ZzZ… (or zZz…) for controverse windings; ZZZ… (or zzz…) for equiverse windings;
– angle α_{cph} among the first coils of consecutive cycle-phases of the same layer (called parent coils): $\alpha_{cph} = (N_{tcph} + 1/N_{ph}) \cdot 180^e$: the evaluation of α_{cph} (to be reduced within 0^e – 360^e) allows to assign the parent coils to the phases;
– as known, for 3-phase and 2-phase windings, the following phasor sequences are valid respectively: 6-phasor sequence: AcBaCb; 4-phasor sequence: ABab (with phase angle displacements of 60^e and 90^e respectively);
– consider as defined the belonging to a chosen phase (included the winding direction) of the parent coil of a first cycle-phase (whose name is X, among those of the phasorial diagram; - in fig.1: A, first left coil of the upper layer -): the parent coil of the adjacent cycle-phase is assigned to the phase whose name Y is that of the phasor which, in the considered phasorial sequence, has an angular distance equal to α_{cph} electrical degrees from X (c in the upper layer of fig.1, where $\alpha_{cph} = 60^e$); similar attribution must be done for the parent coils of all the subsequent cycle-phases of the same layer (always according to the chosen rotating direction along the phasor sequence, CW in phasor sequences and in fig.1);
– the other layer is obtained by simply copying the previous layer, displaced by N_{ts}; it can be shown that the choice of N_{ts} that optimises the E.M.F. waveform is that nearest to $N_{ts.opt} = N_{tcph}/2$ (if N_{ts} is even, the layers are the same also as concerns the coil winding direction; if N_{ts} is odd, the layers are equal, with inverted winding directions).

For 3-phase windings, Table 1 shows some example values of N_{tc} and of N_{mci}, N_{mcs}; also the corresponding successions $S_{cph.i}$ and $S_{cph.s}$ are given for the parent coils of 2 adjacent cycles of one layer (S_{cph} can be called succession of the parent coils of the cycle-phases). Similar Tables can be adopted for other number of phases.

Further important properties characterise tooth-coil machines:

– considering that the N° of slots equals the N° of teeth, the N° of slots/(pole-phase) q of a tooth-coil machine is given by: $q = N_{tc} / (N_{mc} \cdot N_{ph}) \Rightarrow q = (1 \pm 1/N_{mc}) \cdot (1/N_{ph}) \approx 1/N_{ph}$; thus, a 3-phase machine has: $q \approx 0.33$;
– it can be shown that the winding factor k_w of a 3-phase tooth-coil machine (with double-layer windings, N_{ccph} coils/(cycle-phase)), N_{tcph} teeth/(cycle-phase) and layer displacement of N_{ts} teeth) equals the product of a distribution factor k_d times a displacement factor k_s; for the j^{th} E.M.F. harmonic of the phase winding (j = 1, 3, 5,…), we have:

$$k_{w_j} = k_{d_j} \cdot k_{s_j}, \quad \text{with} \quad k_{d_j} = \frac{\sin(j \cdot \pi/6)}{N_{ccph} \cdot \sin\left[\left(j/N_{ccph}\right) \cdot \pi/6\right]},$$

$$k_{s_j} = \cos\left(j \cdot \left(N_{ts}/N_{tcph}\right) \cdot \pi/6\right);$$

as known, a traditional machine, with two layers, distributed windings, q slots/(pole-phase) and coil pitch shortening of c_a slots, exhibits a winding factor f_a equal to the product of a distribution factor f_d times a pitch factor f_p, with expressions exactly corresponding to the previous ones, provided that we associate N_{ccph} with q, and N_{ts} with c_a: the difference is that, with a traditional machine, a good E.M.F. waveform quality and a low force (torque) ripple can be obtained by adopting armature structures with a N° of slots/(pole-phase) q around 5-6, while a tooth coil machine exhibits similar performance quality with q values practically equal to 0.33;
– the incremental spatial shift among field poles and armature teeth leads to a practical absence of disturbances due to slotting (E.M.F. waveform distortion and oscillating forces - torques -); in the traditional PM machines the cogging effect takes place even without armature feeding, so that in order to reduce it, a suited skewing is required among slots and poles of the faced structures.

TABLE 1. COMBINATIONS OF N_{tc} AND N_{mc} FOR 3-PHASE WINDINGS, FOR SOME N_{tcph} VALUES; SUCCESSIONS S OF PARENT COILS.

3-phase controverse windings (all teeth wound):						
Ntcph	*Nccph*	*Ntc*	*Nmci*	*Scph.i*	*Nmcs*	*Scph.s*
2	2	6	5	AcBaCb	7	AbCaBc
3	3	9	8	ACBACB	10	ABCABC
4	4	12	11	AcBaCb	13	AbCaBc
5	5	15	14	ACBACB	16	ABCABC
6	6	18	17	AcBaCb	19	AbCaBc

3-phase equiverse windings (alternatively wound teeth):						
Ntcph	*Nccph*	*Ntc*	*Nmci*	*Scph.i*	*Nmcs*	*Scph.s*
2	1	6	5	AcBaCb	7	AbCaBc
4	2	12	11	AcBaCb	13	AbCaBc
6	3	18	17	AcBaCb	19	AbCaBc
8	4	24	23	AcBaCb	25	AbCaBc
10	5	30	29	AcBaCb	31	AbCaBc

3. LINEAR ACTUATORS

Even if a linear actuator could consist of a long armature stator, faced to a short PM slider, in practice this disposition is rarely adopted, because of the complications connected to the subdivision of the stator winding into separated sections and to their sequential feeding: in fact, this subdivision is aimed to limit winding losses, voltage drops and inverter rating. Thus, in the following, only long PM stator guides and short 3-phase armature sliders will be analysed.

As known, in case of iron-core structures, the normal forces are very high, thus suggesting the use of double-side configurations. Nevertheless, also a single-side disposition will be considered, because its analysis can suggest suitable arrangements of the double-side device, able to limit unwanted forces and waveform distortion, due to end effects.

In order to limit the slider length and to show the device quality even in case of a small N° of teeth, the most simple structure will be studied (N_{tc} = 6, $N_{mc} = N_{tc} + 1 = 7$), equipped with 2 layers displaced by $N_{ts} = N_{tcph}/2 = 1$.

Preliminary FEM analyses (not reported here for brevity) have evidenced that adopting a slider with a number of teeth strictly equal to the wound teeth (6 in our example) implies unsymmetrical phase E.M.F.s and distorted force waveforms; thus, in the following, only sliders equipped with two additional unwound end teeth will be analysed.

Fig.2 and Table 2 illustrate the data of a Single-Side, Double-Layer actuator (SSDL), consisting of 8 teeth: as shown with the dotted lines in fig.2, the slider magnetic structure can be obtained by suitably joining standard E cores.

As known, a classical way to double the thrust, with a simultaneous great lowering of the normal force, consists in simply vertical mirroring the structure of fig.2: even if this choice achieves the desired goals, it does not allow to reduce the detent force (at zero currents), because of the cogging end effects (absent in a rotating device); a first way to obtain a cogging spatial filtering is to apply a 90^e spatial displacement among the two PM side sequences, as shown in the Double-Side, Double-Layer device of fig.3D (DSDL): in it, all the phase coils, suitably rearranged, are series connected; a more practical disposition is the Double-Side, Single-Layer one of fig.3S (DSSL), where the advantages of the double layer winding can be achieved also with one-layer windings/side, by suitably displacing the side winding portions.

Fig.4 shows various FEM simulated time waveforms [8], during translation at constant speed of the SSDL slider of fig. 2 (left) and of the DSDL and DSSL sliders of fig. 3D,S (right), always at f = 20 Hz: upper figures show the zero-current E.M.F. waveforms; middle and lower figures show the normal and tangential force waveforms respectively, at the zero-current (detent force) and with constant d.c. currents (holding force; current values: I_A = 7 A; $I_B = I_C$ = –3.5 A).

By examining the diagrams of fig.4, the following remarks can be made:

– all the E.M.F. waveforms are very close to be perfectly sinusoidal and symmetrical; moreover, the E.M.F.s of the DSDL and DSSL devices are exactly the same, and show a double amplitude compared with that of the SSDL device;
– the normal forces of the SSDL device are very high and always of the same sign, while the normal forces of both the double-side devices are significantly lower and with variable sign, allowing a more favourable bearing sizing;
– the zero-current tangential force F_{to} of the double-side device, greatly lower than the corresponding one of the SSDL device, is very close to zero (in practice, it can be largely referred to the FEM simulation numerical noise);
– the holding tangential force F_{th} developed by the double-side devices is exactly the same, roughly double than that of the SSDL device; moreover, its shape is more similar to a sinusoid than that of the SSDL device, without any appreciable cogging or end effects.

A rough estimation of the operating performance of the DSSL device leads to the following force density quantities: developed thrust per unit slider mass: 45 N/kg; developed thrust per unit total air-gap faced surfaces: 17 kN/m^2. It should be noted that these figures of merit, already interesting, are not referred to an optimised device, thus allowing for significant, further improvements, such as: adoption of PM width wider than the tooth width (thus increasing the air-gap flux density); forced liquid cooling, allowing to increase the current density.

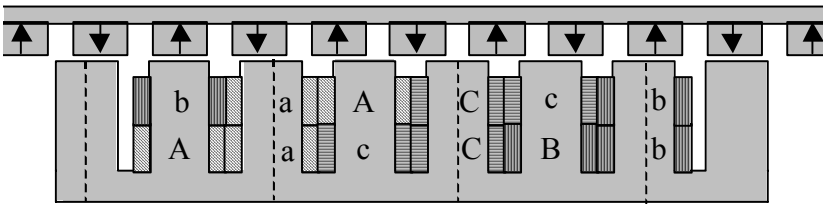

Figure 2. Single-side, double-layer actuator (SSDL), with long stator PM unskewed guide and iron core short slider, (with 3-phase, tooth-coil, windings); slider armature extended to 1 electro-magnetic cycle, including N_{mc}= 7 PMs, N_{tc}= 6 teeth (plus 2 additional unwound end teeth); the slider magnetic structure can be made by joining E transformer standard cores (see dot lines).

TABLE 2. MAIN DATA OF THE ACTUATOR OF FIG.2

tooth pitch, width, height [mm]	18, 12, 18
slider transversal size [mm]	100
slider core yoke [mm]	6
cycle longitudinal extension [mm]	108 = 6 x 18
N° of coils/tooth; N° of turns/coil	2 ; 30
wire diameter [mm]	0.56
coil resistance (at 115 °C) [Ω]	0.73
permanent magnet (PM) material	NdFeB 35
PM remanence; coercitive force	1.23T; 980 kA/m
PM width, height, length [mm]	12 x 5 x 100
permanent magnet pitch [mm]	108/7 = 15.43
slider core sizes [mm]	138 x 24 x 100

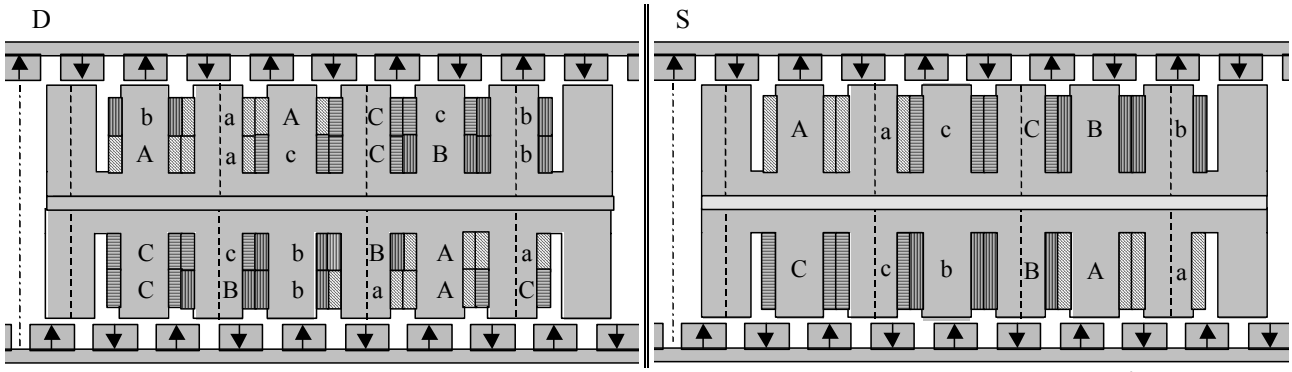

Figure 3. Double-side actuators, with each side characterised by the same magnetic geometry and sizes of fig.2 and Table 2; a 90^e spatial angular displacement is adopted among the two PM side sequences, in order to reduce the end effect detent force; winding wire diameter: 0.56 mm; fig.**D**: DS**D**L slider, with a Double-Layer winding/side (30 turns/coil); fig.**S**: DS**S**L slider, with a Single-Layer winding/side (60 turns/coil).

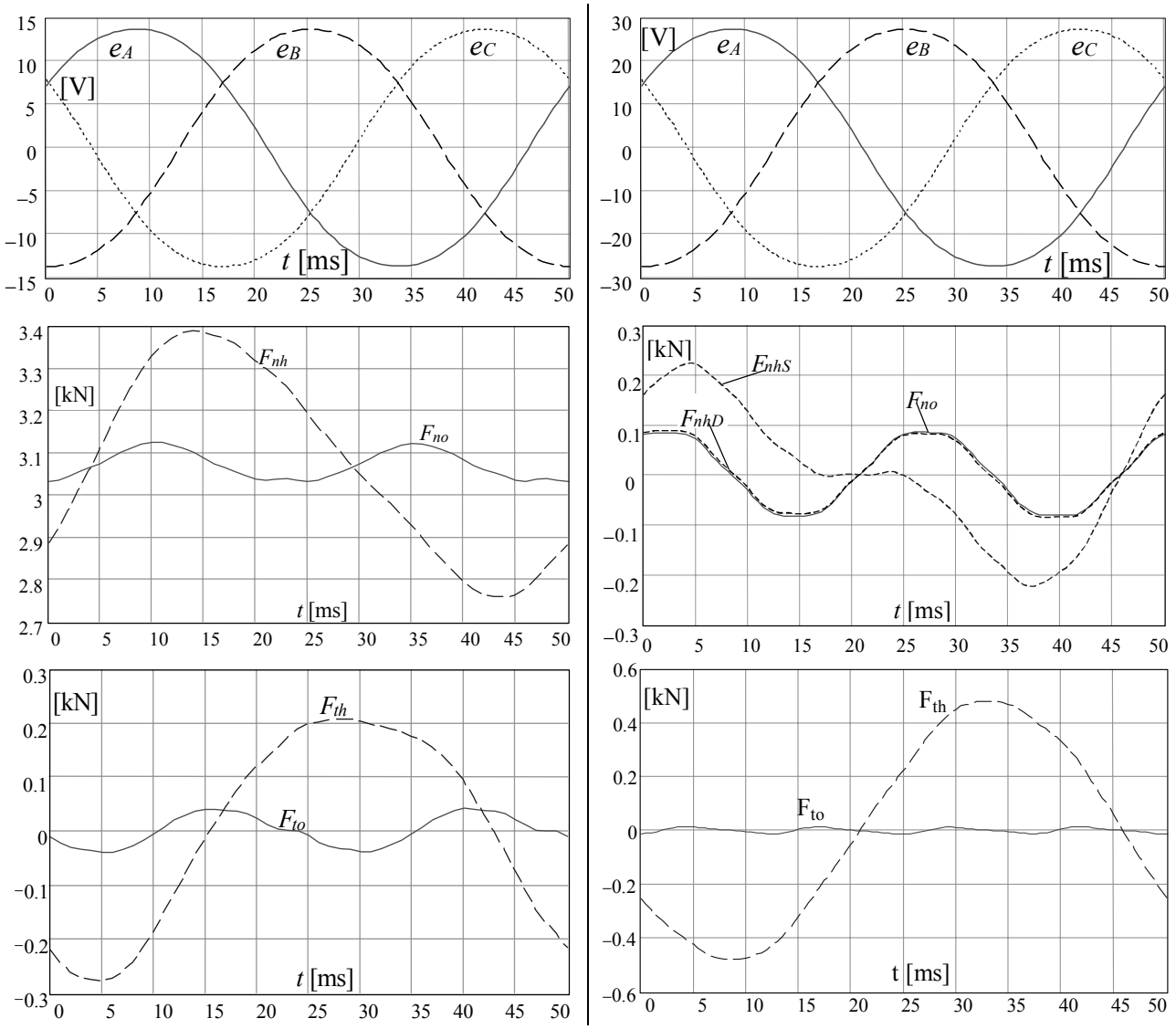

Figure 4. FEM simulated time waveforms [8], during translation at constant speed, always at f = 20 Hz; left diagrams: SSDL device (fig.2); right diagrams: DSDL and DSSL devices (fig.3D,S); upper figures: zero-current E.M.F. waveforms; middle and lower figures: normal and tangential force waveforms respectively (F_n, F_t), at the zero-current (detent forces, F_o) and with d.c. currents (holding force, F_h); I_A =7 A; $I_B = I_C = -3.5$ A).

4. CONCLUSION

The features of the DSSL PM linear actuator make this device very interesting for applications requiring high quality performances, thanks to its great compactness and its ripple free electromechanical performances.

The very simple winding, consisting of just concentrated coils disposed around the armature slider teeth, allows a quick and automated manufacture, with many design opportunities as regards the numbers of wounded teeth within an electromagnetic cycle. No skewing is required, while open slots can be adopted without generating tooth force and E.M.F. harmonics.

Further activities will be carried out, concerning device optimisation and experimental tests on prototypes.

REFERENCES

[1] E. Spooner, A. C. Williamson: British Patent Application 2278738, "Modular Electromagnetic Machine".

[2] P. Lampola, "Electromagnetic Design of an Unconventional Directly Driven Permanent Magnet Wind Generator", *ICEM'98, Proceedings of the XIII International Conference on Electrical Machines,* Istanbul, Turkey, 1998, pp.1705-1710.

[3] M. Lukaniszyn, M. Jagiela, R. Wrobel, "Influence of Magnetic Circuit Modifications on the Torque of a Disc Motor with Co-axial Flux in the Stator", *ICEM'02, Proceedings on CD-ROM of the XV International Conference on Electrical Machines,* Brugge, Belgium, 2002, paper n. 069.

[4] A. Muetze, A. Jack, B. Mecrow, "Alternate Designs of Low Cost Brushless DC Motors using Soft Magnetic Composites", *ibidem*, paper n. 237.

[5] Th. Koch, A. Binder, "Permanent Magnet Machines with Fractional Slot Winding for Electric Traction", *ibidem*, paper n. 369.

[6] W. R. Canders, F. Laube, H. Mosebach, "PM Excited Polyphase Synchronous Machines with Single-Phase Segments. Featuring Simple Tooth Coils, *ibidem*, paper n. 610.

[7] A. Di Gerlando, M. Ubaldini: Italian Patent Application MI2002A 001186, "Synchronous Electrical Machine with Concentrated Coils", May 31st, 2002; international PCT Patent pending.

[8] Maxwell 2D Transient FEM code, 8.0.27 Version, Ansoft Corporation, Pittsburgh, PA.